

SCIENTIFIC REPORTS



OPEN

Functional relationship of *AtABCG21* and *AtABCG22* in stomatal regulation

Takashi Kuromori¹, Eriko Sugimoto¹, Haruka Ohiraki², Kazuko Yamaguchi-Shinozaki² & Kazuo Shinozaki¹

Stomatal regulation is important for water transpiration from plants. Stomatal opening and closing are controlled by many transporter proteins in guard cells. *AtABCG22* is a member of the ATP-binding cassette (ABC) transporters and is a stomatal regulator; however, the function of *AtABCG22* has not yet been determined fully, although a mutant phenotype included a significant effect on stomatal status. Here, we further investigated the function of the *AtABCG22* gene and its functional relationships with other subfamily genes. Among close family members, we found a functional relationship of stomatal phenotypes with *AtABCG21*, which is also expressed specifically in guard cells. Based on an analysis of double mutants, adding the *atabcg21* mutation to *atabcg22* mutant partially suppressed the open-stomata phenotype of *atabcg22*. Multiple-mutant analyses indicated that this suppression was independent of abscisic acid signaling in guard cells. We also found that *atabcg22* mutant showed a unique time course-dependent phenotype, being defective in maintenance of stomatal status after initial stomatal opening elicited by light signaling. The function of *AtABCG22* and its relationship with *AtABCG21* in stomatal regulation are considered.

Stomata consist of a pair of guard cells, a unique cell type with an important role in regulating water transpiration from plant surfaces. Many regulators in guard cells have been shown to function in the closing or opening of stomata. For example, *open stomata1 (ost1)/snf1-related protein kinases 2e (srk2e)* mutants defective in abscisic acid (ABA) signaling have been isolated as major open-stomata (OST) mutant due to the inability to close its stomata^{1,2}. Additionally, cell membrane transporter proteins are important as stomatal regulators^{3,4}, because guard cells are isolated symplastically from neighboring cells⁵⁻⁷.

The superfamily of ATP-binding cassette (ABC) transporters is one of the most abundant protein families in nature. These proteins are broadly conserved from prokaryotes to higher eukaryotes in all phyla that use energy to transport substrates in an ATP-dependent manner against concentration gradients. Plant genomes, in particular, have large ABC families of more than 100 genes, indicating that some ABC transporters likely have important roles in plant-specific developmental and environmental responses^{8,9}.

In plant ABC subfamilies, the ABCG subfamily is the largest, composed of both 'half-size' and 'full-size' transporters. In *Arabidopsis*, 28 gene members have been classified as *AtABCG* half-size transporters⁸, about half of which have been described in the literature. For example, *AtABCG1* and *AtABCG16* are required for pollen nexine layer formation, and *AtABCG2*, *AtABCG6*, and *AtABCG20* are required for suberin barriers¹⁰⁻¹². *AtABCG9* is involved in pollen coat maturation, related to steryl glycosides, in concert with a full-size transporter, *AtABCG31*¹³. *AtABCG11*, *AtABCG12*, and *AtABCG13* are involved in transporting precursors of wax and cutin to the epidermis¹⁴⁻¹⁸. *AtABCG14* controls the root-to-shoot translocation of cytokinins and plant development¹⁹⁻²¹. *AtABCG19* has a role in antibiotic resistance²². *AtABCG25* is involved in ABA transport and responses²³. *AtABCG26* is essential for exine formation, by transporting polyketide sporopollenin precursors²⁴⁻²⁹. Most of these transporters are consequently related to roles in maintaining water content or in prohibiting water loss from plant bodies or pollen cells.

In addition to the members above, we previously isolated *AtABCG22*, which also functions in retaining water in plants³⁰. Mutant *AtABCG22* plants show increased water transpiration and drought susceptibility, suggesting a relationship with ABA function. However, we additionally found enhanced phenotypes of *atabcg22* mutant which

¹RIKEN Center for Sustainable Resource Science, Wako, Saitama, 351-0198, Japan. ²Graduate School of Agricultural and Life Sciences, The University of Tokyo, Bunkyo-ku, Tokyo, 113-8657, Japan. Correspondence and requests for materials should be addressed to T.K. (email: takashi.kuromori@riken.jp)

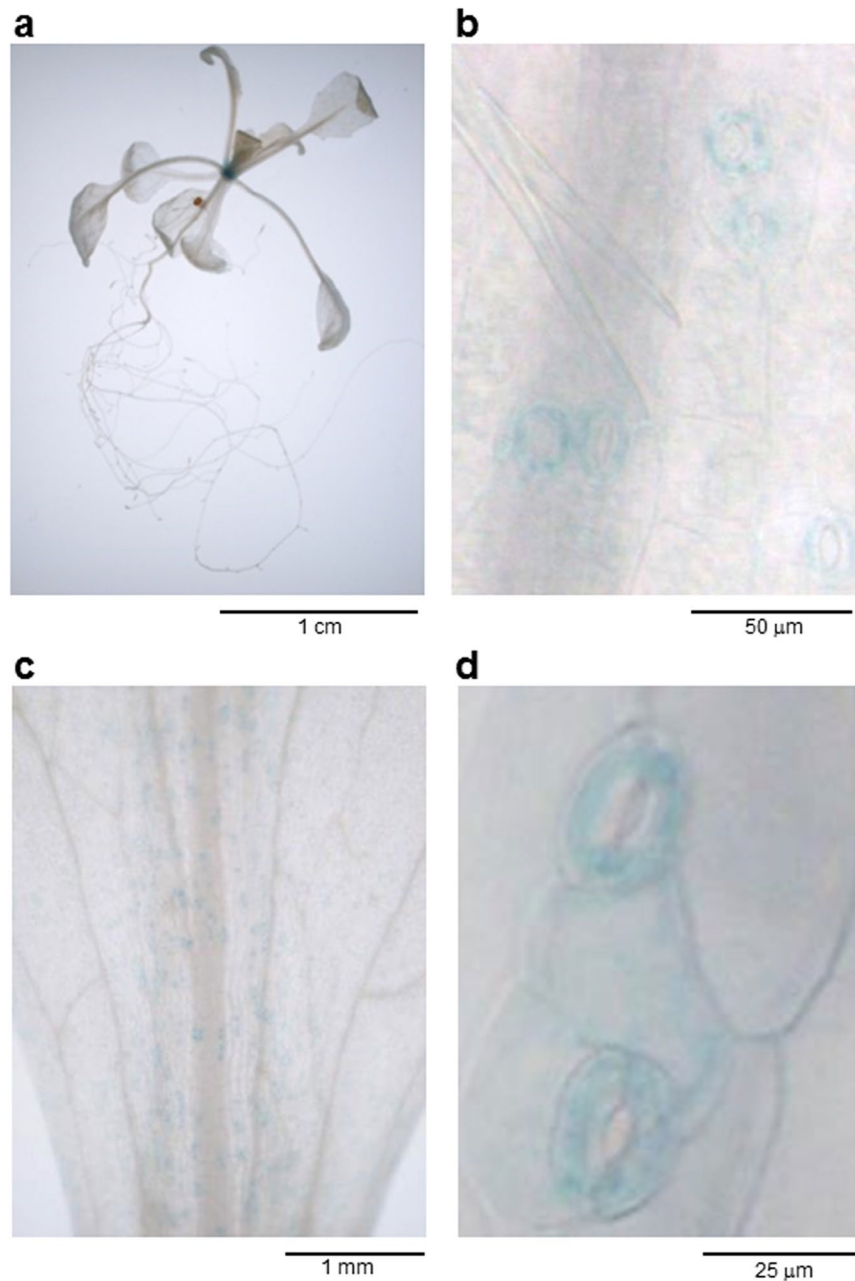


Figure 1. *AtABCG21* gene expression patterns based on GUS staining. (a) Whole seedling of a 2-week-old plant. (b) Magnified image of a leaf in (a). (c) Leaf of a 5-week-old plant. (d) Magnified image of (c). In both growth stages, guard cells were mostly stained.

exhibited an additive effect to ABA signaling or ABA biosynthesis, so that the function of *AtABCG22* in guard cells remains to be determined.

Here, we show that *AtABCG22* has a functional relationship with *AtABCG21*, which is a closely related but as yet unanalyzed member of the ABCG subfamily in *Arabidopsis*. We also examined an *atabcg22* mutant phenotype involved in stomatal regulation.

Results

***AtABCG21* gene expression patterns in plant organs.** We previously reported *AtABCG22* was involved in stomatal regulation, because *atabcg22* mutants that exhibited a typical open-stomata (OST) phenotype³⁰. To study the relationship between *AtABCG22* and other ABCG members that were closely related based on a phylogenetic tree^{17,30}, we focused one of the family members, *AtABCG21*. To investigate the gene expression patterns of *AtABCG21* in wild-type (WT) tissues, we used ~2 kb of the *AtABCG21* promoter region (*pAtABCG21*) to drive expression of a β -glucuronidase (*GUS*) reporter gene. In *pAtABCG21::GUS* transgenic plants, *GUS* activity of the transformants was detected in guard cells of seedlings, but not in roots (Fig. 1a,b). The leaf surface

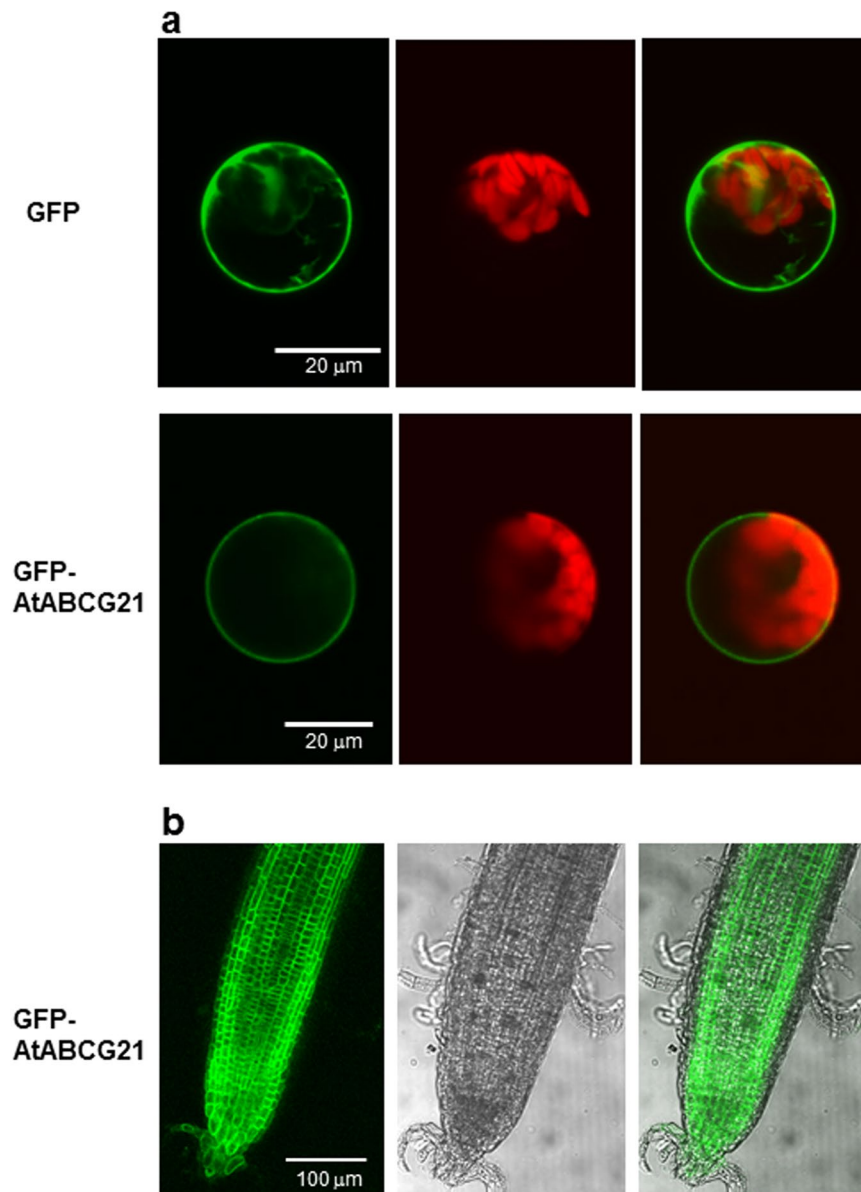


Figure 2. Subcellular localization of AtABC21. (a) Transient expression of GFP protein and GFP-AtABC21 fusion protein in *Arabidopsis* protoplasts. The left panels show images of GFP fluorescence, the middle panels are images of chloroplast autofluorescence, and the right panels are merged images. (b) Subcellular localization of GFP-AtABC21 fusion proteins in root cells in 35Spro:GFP-AtABC21 transgenic plants. The left panel shows an image of GFP fluorescence, the middle panel is a bright-field image, and the right panel is a merged image.

was also stained in adult plants, and GUS staining was detected primarily in guard cells in magnified images (Fig. 1c,d). This gene expression pattern was similar to that of *AtABC22*³⁰, suggesting a guard-cell function for AtABC21.

Subcellular localization of the AtABC21 protein. We showed previously that AtABC22 was localized to the cell membrane in plant cells³⁰. To study the subcellular localization of AtABC21, we made a construct that expressed green fluorescent protein (GFP) fused to AtABC21 protein under the control of the Cauliflower mosaic virus 35S promoter. The *AtABC21* open reading frame was placed downstream of 35S::GFP. The 35S::GFP-AtABC21 recombinant gene was expressed transiently in *Arabidopsis* protoplasts. Subcellular localization of the fusion protein was visualized by confocal imaging of green fluorescence in protoplast cells. The green fluorescence of the GFP-AtABC21 recombinant protein was present around the cell surface (Fig. 2a). Additionally, we transformed the 35S::GFP-AtABC21 recombinant vector into *Arabidopsis* plants. GFP-AtABC21 recombinant protein fluorescence was observed clearly around the cell surface in root cells of the transgenic plants (Fig. 2b). These results indicated that AtABC21 was localized to the cell membrane.

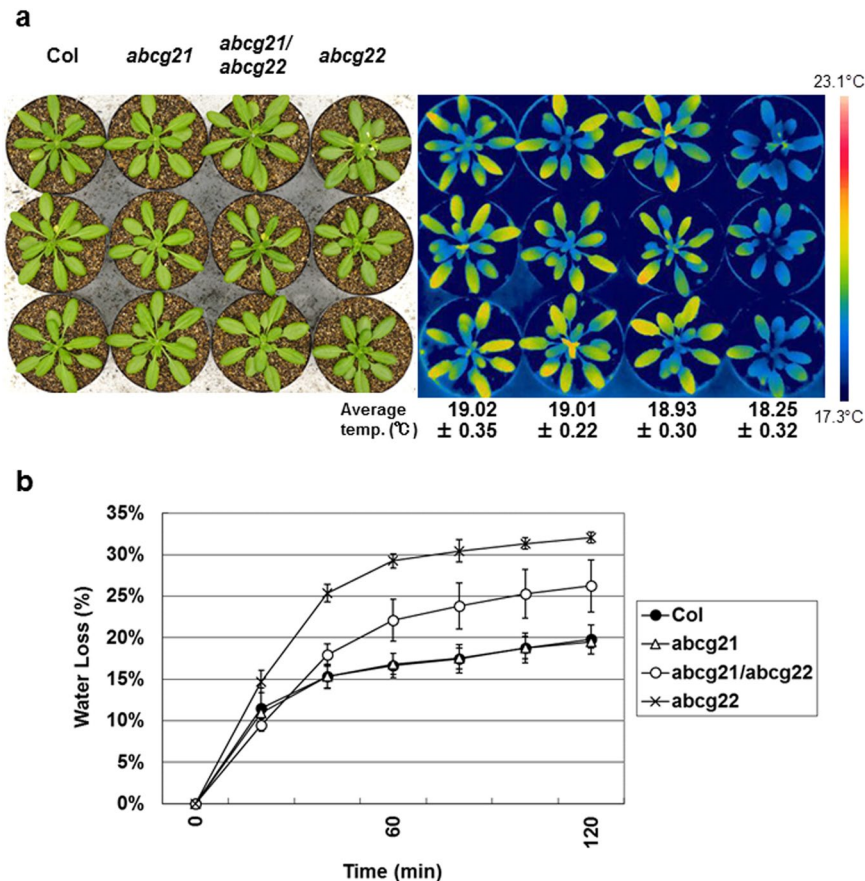


Figure 3. Functional relationship between *atabcg21* and *atabcg22* in transpiration phenotypes. (a) Thermal images of *atabcg21*, *atabcg22*, and double-mutant plants. Rosette leaves of 5-week-old wild-type plants (Col), *atabcg21* mutant plants (*atabcg21*), double-mutant plants (*atabcg21/atabcg22*), and *atabcg22* mutant plants (*atabcg22*) were imaged with a visible-light camera (left panel) and an infrared thermography device (right panel). Average temperatures are shown with SD under each line of thermal images. (b) Transpiration ratio of *atabcg21*, *atabcg22*, and double-mutant plants. Water loss in detached rosette leaves of 5-week-old plants was determined as a percentage of the initial fresh weight. Values are shown as means \pm SD of the three independent plants photographed in (a).

Suppression effect of an *atabcg21* mutation on an *atabcg22* mutant phenotype. We previously reported that the leaf temperature of *atabcg22* mutant plants was lower than that of WT plants under normal growth conditions, because of the OST phenotype³⁰. To investigate the functional relationship between *AtABCG21* and *AtABCG22*, we isolated a homozygous T-DNA insertional mutant on *AtABCG21* by genotyping (Supplemental Fig. S1a), and confirmed this line was a gene knockout mutant (Supplemental Fig. S1b). We did not find any significant phenotype related to water transpiration for the *atabcg21* mutant plants (Supplemental Fig. S1c,d, Fig. S2a,b). However, when we crossed an *atabcg21* mutant with an *atabcg22* mutant to produce double mutants, we found that the leaf temperature of *atabcg21/atabcg22* double-mutant plants was similar to that of WT plants, indicating that transpiration was lower in the leaves of the double mutants than the *atabcg22* mutants (Fig. 3a). This was confirmed by the results of a water-loss experiment in which the rate of weight loss from detached leaves of the double-mutant plants was slower than that from detached leaves of *atabcg22* mutants, partially recovered to WT plants or *atabcg21* single mutants (Fig. 3b). These results indicated that the *atabcg21* mutation partially suppressed the OST phenotype of *atabcg22* mutants, suggesting a functional relationship between *AtABCG21* and *AtABCG22* in stomatal regulation.

The *atabcg21* mutation does not suppress *srk2e* and *nced3* mutant phenotypes. Next, we investigated whether the *atabcg21* mutation could suppress the phenotype of other OST-type mutants, particularly those related to ABA biosynthesis or ABA signaling. We crossed *atabcg21* mutant plants with *srk2e* or *nine-cis-epoxycarotenoid dioxygenase3* (*nced3*) mutants to produce each double mutant. *SRK2E* encodes a kinase involved in cellular ABA signaling in guard cells and *NCED3* encodes a key enzyme in ABA biosynthesis^{1,2,31}. Single mutants of *srk2e* or *nced3* are typical OST-type mutants, and showed lower leaf temperatures and accelerated transpiration from leaves, compared with WT plants (Supplemental Figs S1,S2). The leaf temperature and transpiration rates of the *atabcg21/srk2e* and *atabcg21/nced3* double mutants were almost the same as those of the *srk2e* and *nced3* single mutants, respectively (Supplemental Figs S1,S2). These results indicated that the *atabcg21*

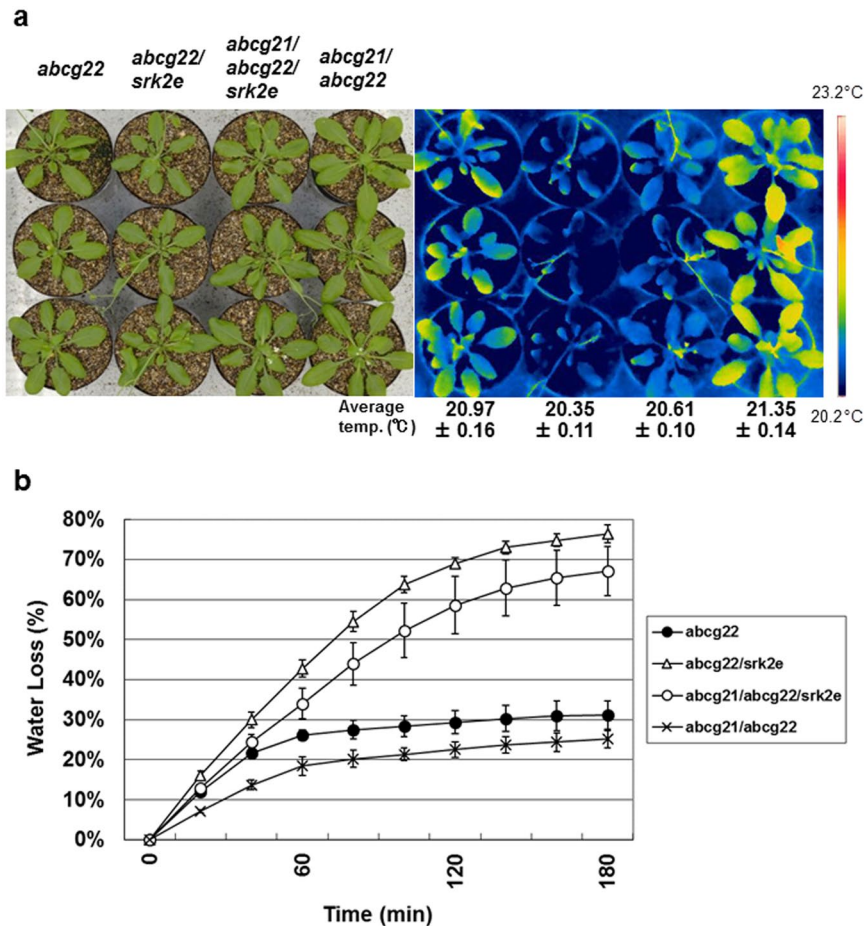


Figure 4. Suppression phenotype of *atabcg21* on *atabcg22* and an ABA signaling mutant. **(a)** Thermal images of double and triple mutant plants of *atabcg21*, *atabcg22*, and *srk2e*. Rosette leaves of 5-week-old *atabcg22* mutant plants (*abcg22*), *atabcg22/srk2e* double-mutant plants (*abcg22/srk2e*), *atabcg21/atabcg22/srk2e* triple-mutant plants (*abcg21/abcg22/srk2e*), and *atabcg21/atabcg22* double-mutant plants (*abcg21/abcg22*) were imaged with a visible-light camera (left panel) and an infrared thermography device (right panel). Average temperatures are shown with SD under each line of thermal images. **(b)** Transpiration ratio of double and triple mutant plants of *atabcg21*, *atabcg22*, and *srk2e*. Water loss in detached rosette leaves of 5-week-old plants was determined as a percentage of the initial fresh weight. Values are shown as means \pm SD of the three independent plants photographed in (a).

mutation did not generally suppress the phenotype of all OST-type mutants, but may repress *atabcg22* specifically, suggesting a specific relationship with the function of AtABC22.

Phenotypes of multiple-mutant plants with ABA signaling defects. When we first isolated *atabcg22* mutants, we suspected a relationship between AtABC22 function and ABA responses. However, double mutants of *atabcg22* and ABA signaling mutants showed additive effects, so this issue was not resolved³⁰. In the process of investigating whether the suppression effect of the *atabcg21* mutation on the *atabcg22* mutant was dependent on ABA in guard cells, we crossed *atabcg21/atabcg22* double-mutant plants with *srk2e* mutants to produce triple mutants. As reported previously for the enhanced phenotypes of *atabcg22/srk2e*³⁰, the leaf temperature of the triple-mutant plants, including *srk2e*, was lower than that of the *atabcg21/atabcg22* double mutants (Fig. 4a). Notably, the leaf temperature of triple-mutant plants was slightly, but significantly, higher than that of *atabcg22/srk2e* double mutants (Fig. 4a). This result was consistent with that of a water-loss experiment, in which the rate of weight loss from detached leaves of the triple-mutant plants was lower than that from detached leaves of *atabcg22/srk2e* double mutants (Fig. 4b). These results indicated that the *atabcg21* mutation still suppressed the OST phenotype of *atabcg22/srk2e* to some extent, even in a *srk2e* mutant background, having ABA-signaling defects. This suggested that the suppression effect of the *atabcg21* mutation on *atabcg22* mutants may be independent of ABA signaling in guard cells.

Light signal-dependent phenotype of the *atabcg22* mutant. The *atabcg22* mutant plants exhibited lower leaf temperatures and increased water loss, indicating elevated transpiration through an effect on stomatal regulation. To address the function of AtABC22, we measured stomatal conductance over a time course,

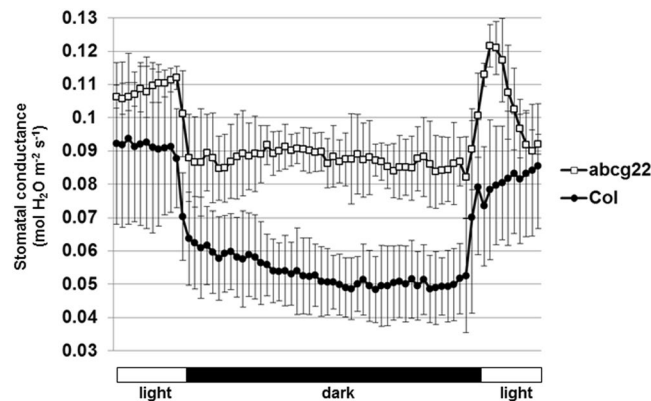


Figure 5. Stomatal conductance in response to changes in light status. Stomatal conductance of wild-type (Col) and *atabcg22* (*atabcg22*) was measured using a gas-exchange system (LI-6400). Data are plotted at 10 min intervals for 12 h, including 8 h of dark, in a conditioned green house. The CO₂ concentration of the air flow was set at 400 ppm during experiments. Values are shown as means \pm SD ($n = 3$).

including light and dark periods. Overall, the stomatal conductance of *atabcg22* mutants was higher than that of WT plants, consistent with having an OST-type phenotype (Fig. 5). That of *atabcg21* mutants was same as WT plants.

In this experiment, we found a unique behavior of *atabcg22* mutants in the initial period of lighting. When the light was turned on, stomatal conductance increased quickly, as in WT plants. However after this increase, it decreased rapidly in *atabcg22* mutants while it stabilized in WT plants (Fig. 5). When the light was turned off, there appeared to be a normal response in *atabcg22* mutants. These results suggest that AtABCG22 may have a function in balancing the stomatal status after light signaling for stomatal opening.

Discussion

When we crossed *atabcg21* and *atabcg22* mutants to generate double mutants, we found that addition of the *atabcg21* mutation partially suppressed *atabcg22* mutant phenotypes (Fig. 3). In case of signal transduction, when the phenotype of the first mutation was suppressed by the addition of the second mutation, it could suggest bypassing the first mutation by the second mutation in the signaling pathway. However, the mutated genes in this case encode transporter proteins, rather than signaling factors. Furthermore, both genes are expressed predominantly in guard cells, and both proteins were shown to be localized to the cell membrane (Figs 1,2). Additionally, the result that *atabcg21* mutations do not repress other OST-type mutants may indicate a specific relationship between AtABCG21 and AtABCG22 (Supplemental Figs S1,S2).

Accordingly, the simplest interpretation would be that the two transporters have opposite activities in transporting the same substrate. Generally, it has been assumed that eukaryotic ABC proteins uniformly transport a substrate present at the side of the membrane where the nucleotide-binding domain is located to the other side of a membrane; for example, transporters localized to the cell membrane are usually efflux transporters, moving substrates from the cytosol to the outside. However, recent findings show that at least some plant ABC transporters can also act in the opposite direction, as influx transporters, moving substrates from the apoplastic space to the cytosol^{9,32–34}.

ABA is a strong effector enhancing stomatal closure. Several AtABCG family members have been reported to be ABA-transporting factors^{23,34,35}. AtABCG22 transcripts are enriched by drought treatment even under mild conditions³⁶. We suspected that AtABCG21 and/or AtABCG22 would be related to ABA, but genetic combination of multiple mutations did not show this (Fig. 4). Another experiment showed that the stomatal response to exogenous ABA was intact in *atabcg22* mutants, suggesting that AtABCG22 is not involved in ABA uptake into guard cells directly, although AtABCG22 plays a role in initiating stomatal closure due to reduced air humidity^{37,38}. Targeted substrates of AtABCG21 and AtABCG22 are still unknown and remain to be investigated.

Light, especially blue light, causes positive signaling for stomatal opening³⁹. On the other hand, a report that light-dependent stomatal movement of *ost1-2*, an allele of *srk2e*, appeared to be unaffected suggested that light-induced stomatal opening is essentially independent of ABA signaling⁴. In our time-course measurements, we found that *atabcg22* mutant plants could actually respond to light, but then showed rapid attenuation of stomatal opening (Fig. 5). When the light was turned on, cellular light-induced signaling in guard cells was triggered instantly, followed by stomatal opening⁴⁰. Based on the time course-dependent phenotype of the *atabcg22* mutant, AtABCG22 may have a unique function in establishing stable stomatal status in the initial hour after light exposure.

Methods

Plant materials and observations. Plants were grown in soil under well-watered conditions at $22 \pm 2^\circ\text{C}$ and 60–70% relative humidity under a 16/8-h light/dark cycle. The *atabcg21* mutant was a T-DNA-tagged mutant obtained from the Arabidopsis Biological Resource Center (SAIL_786_G09). The *atabcg22* mutant used in this study was reported previously as the *atabcg22-2* (*salk_113844*) allele, and the *srk2e* and *nced3* mutants have been described previously³⁰.

Thermal images were captured using an infrared thermography device (T620; FLIR). Average temperatures were calculated by FLIR Tools. Water-loss experiments were performed using rosette leaves detached from 5-week-old plants, as described previously³⁰.

Visualization of expression sites by GUS staining. For *AtABCG21* promoter-driven GUS expression lines, a 2-kb *AtABCG21* promoter region was amplified using KOD plus polymerase (Toyobo) with the primers *AtABCG21pro_Fw* (5'-CACCGACACCTAAACAAATAGACTTTCGTGA-3') and *AtABCG21pro_Rv* (5'-CTAGAGAAGGAAAGAGAGATAG-3'), cloned into the pENTR/D-TOPO vector (Invitrogen), and then integrated into the GUS-fusion vector, pBGGUS. The plasmid was then electroporated into *Agrobacterium tumefaciens* to generate transgenic plants by floral dipping. GUS staining and observation of GUS-stained plants were performed as described previously³⁰.

Subcellular localization of AtABCG21. Transient expression assays using mesophyll protoplasts from *Arabidopsis* were performed as described previously⁴¹. To build the 35S::GFP-*AtABCG21* construct, a fragment of the *AtABCG21* coding region was amplified by PCR from *Arabidopsis* cDNA with the primer set *AtABCG21_Fw_EcoRV* (5'-AACGATATCATGATGCCTCCTAATGAGCA-3') and *AtABCG21_Rv_NotI* (5'-ATAGCGGCCGCTCACAAAGTTCCTTAGAGCTA-3'). The amplified fragment was ligated between the *EcoRV* and *NotI* sites of the pGKX-NsGFP vector⁴². The same vectors were electroporated into *Agrobacterium* to generate transgenic plants.

Gas exchange measurements. Stomatal conductance was assayed in rosette leaves of 5- to 7-week-old wild-type and *atabcg22* plants using a portable gas exchange system (LI-6400; LI-COR). The air flow was set to 200 $\mu\text{mol s}^{-1}$, and the humidity of the air was not regulated, but the CO_2 concentration of the air was controlled at 400 ppm using a CO_2 cylinder during the experiments.

References

1. Mustilli, A. C., Merlot, S., Vavasseur, A., Fenzi, F. & Giraudat, J. Arabidopsis OST1 protein kinase mediates the regulation of stomatal aperture by abscisic acid and acts upstream of reactive oxygen species production. *Plant Cell* **14**, 3089–3099 (2002).
2. Yoshida, R. *et al.* ABA-activated SnRK2 protein kinase is required for dehydration stress signaling in Arabidopsis. *Plant Cell Physiol* **43**, 1473–1483 (2002).
3. Pandey, S., Zhang, W. & Assmann, S. M. Roles of ion channels and transporters in guard cell signal transduction. *FEBS Lett.* **581**, 2325–2336 (2007).
4. Kim, T. H., Böhmer, M., Hu, H., Nishimura, N. & Schroeder, J. I. Guard cell signal transduction network: advances in understanding abscisic acid, CO_2 , and Ca^{2+} signaling. *Annu. Rev. Plant Biol.* **61**, 561–591 (2010).
5. Galatis, B. & Mitrakos, K. The ultrastructural cytology of the differentiating guard cells of *vigna sinensis*. *Amer. J. Bot.* **67**, 1243–1261 (1980).
6. Wille, A. C. & Lucas, W. J. Ultrastructural and histochemical studies on guard cells. *Planta* **160**, 129–142 (1984).
7. Palevitz, B. A. & Hepler, P. K. Changes in dye coupling of stomatal cells of *Allium* and *Commelina* demonstrated by microinjection of Lucifer yellow. *Planta* **164**, 473–479 (1985).
8. Rea, P. A. Plant ATP-binding cassette transporters. *Annu. Rev. Plant Biol.* **58**, 347–375 (2007).
9. Kang, J. *et al.* Plant ABC Transporters. *Arabidopsis Book* **9**, e0153, <https://doi.org/10.1199/tab.0153> (2011).
10. Yadav, V. *et al.* ABCG transporters are required for suberin and pollen wall extracellular barriers in Arabidopsis. *Plant Cell* **26**, 3569–3588 (2014).
11. Yim, S. *et al.* Postmeiotic development of pollen surface layers requires two Arabidopsis ABCG-type transporters. *Plant Cell Rep.* **35**, 1863–1873 (2016).
12. Fedi, F. *et al.* Awake1, an ABC-Type Transporter, Reveals an Essential Role for Suberin in the Control of Seed Dormancy. *Plant Physiol.* **174**, 276–283 (2017).
13. Choi, H. *et al.* The role of Arabidopsis ABCG9 and ABCG31 ATP binding cassette transporters in pollen fitness and the deposition of steryl glycosides on the pollen coat. *Plant Cell* **26**, 310–324 (2014).
14. Pighin, J. A. *et al.* Plant cuticular lipid export requires an ABC transporter. *Science* **306**, 702–704 (2004).
15. Bird, D. *et al.* Characterization of Arabidopsis ABCG11/WBC11, an ATP binding cassette (ABC) transporter that is required for cuticular lipid secretion. *Plant J.* **52**, 485–498 (2007).
16. Panikashvili, D. *et al.* The Arabidopsis *DESPERADO/AtWBC11* transporter is required for cutin and wax secretion. *Plant Physiol.* **145**, 1345–1360 (2007).
17. Ukitsu, H. *et al.* Cytological and biochemical analysis of COF1, an Arabidopsis mutant of an ABC transporter gene. *Plant Cell Physiol.* **48**, 1524–1533 (2007).
18. Panikashvili, D., Shi, J. X., Schreiber, L. & Aharoni, A. The Arabidopsis ABCG13 transporter is required for flower cuticle secretion and patterning of the petal epidermis. *New Phytol.* **190**, 113–124 (2011).
19. Hir, R. *et al.* ABCG9, ABCG11 and ABCG14 ABC transporters are required for vascular development in Arabidopsis. *Plant J.* **76**, 11–824 (2013).
20. Ko, D. *et al.* Arabidopsis ABCG14 is essential for the root-to-shoot translocation of cytokinin. *Proc. Natl. Acad. Sci. USA* **111**, 7150–7155 (2014).
21. Zhang, K. *et al.* Arabidopsis ABCG14 protein controls the acropetal translocation of root-synthesized cytokinins. *Nat. Commun.* **5**, 3274, <https://doi.org/10.1038/ncomms4274> (2014).
22. Mentewab, A. & Stewart, C. N. Jr. Overexpression of an Arabidopsis thaliana ABC transporter confers kanamycin resistance to transgenic plants. *Nat. Biotechnol.* **23**, 1177–1180 (2005).
23. Kuromori, T. *et al.* ABC transporter AtABCG25 is involved in abscisic acid transport and responses. *Proc. Natl. Acad. Sci. USA* **107**, 2361–2366 (2010).
24. Quilichini, T. D., Friedmann, M. C., Samuels, A. L. & Douglas, C. J. ATP-binding cassette transporter G26 is required for male fertility and pollen exine formation in Arabidopsis. *Plant Physiol.* **154**, 678–690 (2010).
25. Xu, J. *et al.* The ABORTED MICROSPORES regulatory network is required for postmeiotic male reproductive development in Arabidopsis thaliana. *Plant Cell* **22**, 91–107 (2010).
26. Choi, H. *et al.* An ABCG/WBC-type ABC transporter is essential for transport of sporopollenin precursors for exine formation in developing pollen. *Plant J.* **65**, 181–193 (2011).
27. Dou, X. Y. *et al.* WBC27, an adenosine tri-phosphate-binding cassette protein, controls pollen wall formation and patterning in Arabidopsis. *J. Integr. Plant Biol.* **53**, 74–88 (2011).

28. Kuromori, T., Ito, T., Sugimoto, E. & Shinozaki, K. *Arabidopsis* mutant of AtABCG26, an ABC transporter gene, is defective in pollen maturation. *J. Plant Physiol.* **168**, 2001–2005 (2011).
29. Quilichini, T. D., Samuels, A. L. & Douglas, C. J. ABCG26-mediated polyketide trafficking and hydroxycinnamoyl spermidines contribute to pollen wall exine formation in *Arabidopsis*. *Plant Cell* **26**, 4483–4498 (2014).
30. Kuromori, T., Sugimoto, E. & Shinozaki, K. *Arabidopsis* mutants of AtABCG22, an ABC transporter gene, increase water transpiration and drought susceptibility. *Plant J.* **67**, 885–894 (2011).
31. Iuchi, S. *et al.* Regulation of drought tolerance by gene manipulation of 9-cis-epoxycarotenoid dioxygenase, a key enzyme in abscisic acid biosynthesis in *Arabidopsis*. *Plant J.* **27**, 325–333 (2001).
32. Shitan, N. *et al.* Involvement of CjMDR1, a plant multidrug-resistance-type ATP-binding cassette protein, in alkaloid transport in *Coptis japonica*. *Proc. Natl. Acad. Sci. USA* **100**, 751–756 (2003).
33. Lee, M. *et al.* The ABC transporter AtABC14 is a malate importer and modulates stomatal response to CO₂. *Nat. Cell Biol.* **10**, 1217–1223 (2008).
34. Kang, J. *et al.* PDR-type ABC transporter mediates cellular uptake of the phytohormone abscisic acid. *Proc. Natl. Acad. Sci. USA* **107**, 2355–2360 (2010).
35. Kang, J. *et al.* Abscisic acid transporters cooperate to control seed germination. *Nat. Commun.* **6**, 8113, <https://doi.org/10.1038/ncomms9113> (2015).
36. Jammes, F. *et al.* Acetylated 1,3-diaminopropane antagonizes abscisic acid-mediated stomatal closing in *Arabidopsis*. *Plant J.* **79**, 322–333 (2014).
37. Merilo, E., Jalakas, P., Kollist, H. & Brosché, M. The role of ABA recycling and transporter proteins in rapid stomatal responses to reduced air humidity, elevated CO₂, and exogenous ABA. *Mol. Plant* **8**, 657–659 (2015).
38. Merilo, E. *et al.* Abscisic acid transport and homeostasis in the context of stomatal regulation. *Mol. Plant* **8**, 1321–1333 (2015).
39. Briggs, W. R. & Huala, E. Blue-light photoreceptors in higher plants. *Annu. Rev. Cell Dev. Biol.* **15**, 33–62 (1999).
40. Shimazaki, K., Doi, M., Assmann, S. M. & Kinoshita, T. Light regulation of stomatal movement. *Annu. Rev. Plant Biol.* **58**, 219–247 (2007).
41. Yamada, K. *et al.* Functional analysis of an *Arabidopsis thaliana* abiotic stress-inducible facilitated diffusion transporter for monosaccharides. *J. Biol. Chem.* **285**, 1138–1146 (2010).
42. Qin, F. *et al.* *Arabidopsis* DREB2A-interacting proteins function as RING E3 ligases and negatively regulate plant drought stress-responsive gene expression. *Plant Cell* **20**, 1693–1707 (2008).

Acknowledgements

We thank the RIKEN Center for Sustainable Resource Science (CSRS) for transgenic plant and sequencing support. This work was supported by JSPS KAKENHI Grant Number 17K07458 (to TK), and the Kurata Grant awarded by the Kurata Memorial Hitachi Science and Technology Foundation (to TK).

Author Contributions

T.K. designed the experiments, analyzed the data and wrote the article with contributions of all the authors; E.S. and H.O. provided technical assistance and performed the experiments; K.Y.-S. and K.S. supervised and complemented the writing.

Additional Information

Supplementary information accompanies this paper at <https://doi.org/10.1038/s41598-017-12643-6>.

Competing Interests: The authors declare that they have no competing interests.

Publisher's note: Springer Nature remains neutral with regard to jurisdictional claims in published maps and institutional affiliations.



Open Access This article is licensed under a Creative Commons Attribution 4.0 International License, which permits use, sharing, adaptation, distribution and reproduction in any medium or format, as long as you give appropriate credit to the original author(s) and the source, provide a link to the Creative Commons license, and indicate if changes were made. The images or other third party material in this article are included in the article's Creative Commons license, unless indicated otherwise in a credit line to the material. If material is not included in the article's Creative Commons license and your intended use is not permitted by statutory regulation or exceeds the permitted use, you will need to obtain permission directly from the copyright holder. To view a copy of this license, visit <http://creativecommons.org/licenses/by/4.0/>.

© The Author(s) 2017